Silencing of CEBPB-AS1 modulates CEBPB expression and resensitizes BRAF-inhibitor resistant melanoma cells to vemurafenib

Linda Vidarsdottir[a], Rita Valador Fernandes[a,b], Vasilios Zachariadis[a], Ishani Das[a], Elin Edsbäcker[a], Ingibjorg Sigvaldadottir[a], Alireza Azimi[a,c], Veronica Höiom[a], Johan Hansson[a], Dan Grandér[a,*], Suzanne Egyházi Brage[a] and Katja Pokrovskaja Tamm[a]

Introduction of targeted therapy in the treatment of metastatic cutaneous malignant melanoma (CMM) has improved clinical outcome during the last years. However, only in a subset of the CMM patients, this will lead to long-term effects. CEBPB is a transcription factor that has been implicated in various physiological and pathological processes, including cancer development. We have investigated its prognostic impact on CMM and unexpectedly found that higher *CEBPB* mRNA levels correlated with a longer overall survival. Furthermore, in a small cohort of patients with metastatic CMM treated with BRAF-inhibitors, higher levels of *CEBPB* mRNA expression in the tumor cells prior treatment correlated to a longer progression-free survival. We have characterized an overlapping antisense transcript, *CEBPB-AS1,* with the aim to investigate the regulation of CEBPB expression in CMM and its impact on BRAF-inhibitor sensitivity. We demonstrated that silencing of *CEBPB-AS1* resulted in epigenetic modifications in the CEBPB promoter and in increased *CEBPB* mRNA and protein levels, inhibited proliferation and partially resensitized BRAF-inhibitor resistant CMM cells to this drug-induced apoptosis. Our data suggest that targeting *CEBPB-AS1* may represent a valuable tool to sensitize CMM cells to the BRAF-inhibitor-based therapies. *Melanoma Res* 30: 443–454 Copyright © 2020 The Author(s). Published by Wolters Kluwer Health, Inc.

Melanoma Research 2020, **30**:443–454

Keywords: antisense RNA, BRAF-inhibitor, CEBPB, CEBPB-AS1, cutaneous malignant melanoma

[a]Department of Oncology and Pathology, Karolinska Institutet, Bioclinicum, Solna, [b]Present address: Swiss Institute for Experimental Cancer Research (ISREC), School of Life Sciences, École Polytechnique Fédérale de Lausanne (EPFL), Lausanne, Switzerland and [c]Present address: Department of Immunology, Genetics and Pathology, BMC, Uppsala University, Uppsala, Sweden

Correspondence to Katja Pokrovskaja Tamm, PhD, Karolinska Institutet, Bioclinicum, Visionsgatan 4, 17164 Solna, Sweden
Tel: +46 851773930; e-mail: katja.pokrovskaja@ki.se

*Dan Grandér deceased.

Received 22 October 2019 **Accepted** 12 May 2020

Introduction

Treatment of metastatic cutaneous malignant melanoma (CMM) with chemotherapy has been inefficient and the prognosis is still poor. The use of the BRAF-inhibitors (BRAFi), vemurafenib and dabrafenib, has led to a very efficient tumor regression after treatment in majority of patients with *BRAF* mutant CMM [1]. However, a majority of these patients relapse due to development of resistance that emerges after a median of 6–7 months of single treatment [2] while combining the BRAFi with the MEK inhibitor (downstream of BRAF in the MAPK signaling pathway) prolongs the median progression-free survival (PFS) to 11 months [3]. Multiple molecular events leading to an acquired resistance to the BRAFi/MEKi have been discovered, such as upregulation of receptor tyrosine kinases, downregulation of the tumor suppressor phosphatase and tensin homolog (PTEN) that results in activation of PI3K pathway, amplification of the transcription factor (TF) melanocyte inducing transcription factor, amplifications of mutant BRAF gene and secondary *NRAS* mutations [4]. It is important to understand these molecular mechanisms and also determine novel mechanisms that contribute to BRAFi resistance in CMM in order to potentiate this therapy and overcome or prevent development of resistance.

We have previously described an antisense RNA emanating from PTEN pseudogene, PTENP1-AS, that regulates the PTEN tumor suppressor gene expression [5]. Recently, we have investigated its role in the development of resistance in CMM, and found that TF CCAAT/

Supplemental Digital Content is available for this article. Direct URL citations appear in the printed text and are provided in the HTML and PDF versions of this article on the journal's website, www.melanomaresearch.com.

0960-8931 Copyright © 2020 The Author(s). Published by Wolters Kluwer Health, Inc. DOI: 10.1097/CMR.0000000000000675

enhancer-binding protein beta, CEBPB, is involved in the regulation of transcription of this AS RNA (Vidarsdottir *et al.*, Manuscript under submission). Interestingly, CEBPB can be involved in potentiating drug sensitivity and in ER stress induced cell death in melanoma [6], and this can be connected to the ER stress induced by BRAFi in melanoma cells [7]. CEBPB has been implicated in various cancers; however, it may have opposing roles in tumorigenesis and cell survival, highly dependent on cellular context (reviewed in Ref. 8). CEBPB is a member of the TF CEBP family that can act as dimers with other CEBPs or other TFs, usually leading to activation of gene transcription; however, CEBPs are also capable of transcriptional repression [9,10]. CEBPB has three isoforms, LAP1, LAP2 and LIP, which have different functions that are essential for cells to maintain normal growth and development [11].

In this study, we have analyzed AmpliSEQ data from patients with metastatic CMM and found a longer PFS, in BRAFi-treated patients that have higher levels of *CEBPB* expression in tumor cells analyzed prior to treatment. This prompted us to study the regulation of CEBPB in CMM. Using CMM cell lines, we have characterized an annotated antisense transcript, *CEBPB-AS1*, which negatively regulated *CEBPB* transcription. Knocking down *CEBPB-AS1* led to increased levels of CEBPB transcript and protein, and also led to inhibition of CMM cell proliferation and resensitization of BRAFi resistant cells to BRAFi vemurafenib-induced cell death. Thus, manipulating *CEBPB-AS1* expression may represent a valuable mechanism of resensitizing BRAFi-resistant CMM cells to the mutant BRAFi-based therapy.

Material and methods

Cell culture and cell lines

CMM cell lines A375, SK-MEL-24, SK-MEL-28 (CRL-1619, HTB-71, HTB-72, respectively) and the embryonic kidney HEK293T (CRL-3216) cell line were purchased from ATCC; ESTDAB-049 – from the European Searchable Tumor Cell and Data Bank (Tübingen, Germany), CMM cell line MNT1 [12] was a gift from P.G. Natali, University La Sapienza, Rome, Italy. The resistant A375PR1 cell line was established from A375 as we have described [13]. MNT1-DR100 is a vemurafenib and dabrafenib resistant cell line, derived from the parental cell line MNT1, previously generated by repeated exposure to increasing concentrations of dabrafenib, a selective inhibitor of BRAFV600E [14].

Tumor patients' samples

Tumor samples from 13 CMM patients (Table 1), nine male and four female, taken before start of the treatment with MAPK targeting therapy (BRAFi alone or in combination with MEKi) were collected as fresh frozen fine needle aspirate samples. Median age of the patients was 61 years (range 42–86 years). This study was performed in accordance with the ethical principles in the Helsinki Declaration with ethical approval from the regional ethics committee in Stockholm, Sweden. Informed consent was obtained from all the patients.

RNA isolation and cDNA synthesis

RNA was isolated according to manufacturer´s protocol using the RNA nucleospin kit II (Macherey-Nagel), treated with DNase (Ambion Turbo DNA-free; Life Technologies, Carlsbad, California, USA) and cDNA was generated using M-MLV (Life Technologies) enzyme.

Polyadenylated RNA analysis

MyOne Streptavidin dynabeads (Life Technologies) were blocked in BSA and yeast tRNA and were preloaded with 5′-biotinylated oligonucleotides or control (biotin-362as) oligonucleotides (Integrated DNA Technologies, Coralville, Iowa, USA). DNase pretreated RNA from HEK293T cells was added to the beads and incubated for 2 h at RT. The supernatant containing the poly(A)-depleted RNA fraction was collected and used to generate cDNA. The cDNA was then assessed by semi-quantitative reverse transcription PCR (semi-qRT-PCR).

Table 1 Patient and clinical characteristics, metastatic classification (M-stage) is according to the seventh American Joint American Joint Committee on Cancer (AJCC) staging edition

Patient	Sex	Age	M1 stage	LDH (μKat/L)	Treatment	PFS (days)	OS (days)
1	Male	43	M1b	3	Vemurafenib	966	1091
2	Male	72	M1a	2.6	Vemurafenib	627	833
3	Female	65	M1c	3.8	Vemurafenib	328	350
4	Female	56	M1c	7.2	Vemurafenib	224	507
5	Male	60	M1c	5.3	Vemurafenib	245	1924[a]
6	Male	61	M1c	8	dabrafenib+trametinib	231	346
7	Female	86	M1c	5.3	dabrafenib+trametinib	161	161
8	Male	42	M1c	8.7	Vemurafenib	95	189
9	Male	65	M1c	7	Vemurafenib	84	219
10	Male	66	M1c	3.8	Vemurafenib	70	267
11	Male	50	M1c	4.9	Vemurafenib	35	185
12	Female	64	M1c	30.1	Vemurafenib	42	63
13	Male	52	M1c	3.5	dabrafenib+trametinib	70	395

OS, overall survival; PFS, progression-free survival.
[a]Still alive. LDH values >4.3 μKat/L were considered elevated according to the upper reference level at the Karolinska University Hospital Laboratory.

Actinomycin D treatment

A375PR1 cells were treated with 8 µg/ml actinomycin D (Sigma-Aldrich, saint Louis, Missouri, USA) and RNA was harvested at different time points (0, 2, 6 and 10 h) followed by cDNA synthesis and reverse transcription quantitative PCR (RT-qPCR). Primers are listed in Supplementary Table 1, Supplemental digital content 1, *http://links.lww.com/MR/A233*.

Semi-quantitative reverse transcription PCR

Semi-qRT-PCR was performed with KAPA2G FAST mix (Kapa Biosystems, Wilmington, Massachusetts, USA) according to manufacturer′s instructions under the following cycling conditions: 95°C for 3 minutes, 20–38 cycles of 95°C for 10 seconds, 60°C for 10 seconds and 72°C, finishing at 72°C for 1 minute. Products were run on 2% agarose gels, stained with SYBR safe DNA gel stain (Invitrogen, Carlsbad, California, USA) and documented with Gel Doc EZ System (BioRad, Hercules, California, USA).

Reverse transcription quantitative PCR and primer walk

RT-qPCR was performed with the KAPA SYBR FAST qPCR Master Mix (Kapa Biosystems) on a CFX96 Touch™ Real-Time PCR (Bio-Rad) under following cycling conditions: 95 °C for 3 min, 40 cycles of 95 °C for 3 sec and 60 °C for 30 sec, finishing at 65 ºC for 5 sec. Each PCR was performed in technical duplicate. To determine the 5' end of the *CEBPB-AS1* transcript, the primer walk method was used as we described before.[5]

Cell fractionation and detection of CEBPB and CEBPB-AS1 transcripts

Total RNA extraction and isolation of nuclear and cytoplasmic RNA fractions from A375PR1 cells was performed according to manufacturer's instructions using the PARIS kit (Life Technologies). Extracted RNA fractions, as well as total RNA, were DNase treated prior to cDNA synthesis. *CEBPB* and *CEBPB-AS1* were amplified using a semi-qRT-PCR with corresponding primers (Supplementary Table 1, Supplemental digital content 1, *http://links.lww.com/MR/A233*) and products were run on an agarose gel.

Transfections with Dicer-substrate RNAs

Cells were transfected with Dicer-substrate RNAs (DsiRNAs) (10-20 nM) using Lipofectamine™ 2000 (Life Technologies) according to manufacturer's instructions and harvested 48 hours after transfection. Customized DsiRNAs (see Supplementary Table 2, Supplemental digital content 1, *http://links.lww.com/MR/A233*) were purchased from Integrated DNA Technologies. The RNA expression data from RT-qPCR were normalized to beta-actin and then to siRNA-control-transfected cells.

Protein analysis

Cells were lysed in a modified RIPA lysis buffer (50 mM Tris-HCl, pH 7.4, 1% NP40, 150 mM NaCl, 1 mM EDTA, and 1% glycerol), supplemented with dithiothreitol (DTT), Complete Protease Inhibitor Cocktail (Sigma-Aldrich) and PhosSTOP (Sigma-Aldrich). Protein concentration was determined using Bradford assay (Bio-Rad). 75µg of proteins were loaded on a NuPAGE 4-12% Bis-Tris Gel and transferred onto PVDF Membranes (Invitrogen). Membranes were blocked in 5% milk and immunoblotted overnight at 4 °C with primary antibodies followed by 1 h incubation with HRP-conjugated secondary antibodies. The proteins were detected using Western Lightning–ECL (PerkinElmer). Anti-CEBPB antibodies were from Santa Cruz Biotechnology, Cat# SC-7962), anti-β-actin - from Sigma-Aldrich, Cat# A5441). Band intensity was quantified using Adobe Photoshop Elements Editors. The background was subtracted from each of the values, which were then normalized to the values of loading control.

Chromatin immunoprecipitation

A375 PR1 cells were transfected with siRNAs, and 48 h later crosslinked for 10 min in 0.75% formaldehyde, quenched in 0.125M Glycine for 5min and then lysed in cell lysis buffer (5 mM PIPES, 85 mM KCL and 0.5% NP40) followed by a nuclei lysis buffer (50 nM TRIS-HCI (pH 8), 10 mM EDTA and 1% SDS). Lysates were sonicated using a Bioruptor Sonicator (Diagenode) and incubated overnight at 4°C with either CEBPB (Santa Cruz Biotechnology, Cat#sc-150), H3K27me3 (Upstate/Millipore, Cat#17-622), CTCF (Cell Signaling, Danvers, Massachusetts, USA Cat#2899) or EZH2 (Upstate/Millipore, Cat#07-689) antibodies (4µg/sample). IgG Rabbit (PB644, Merck) was used as a negative control. Salmon Sperm DNA/Protein A Agarose beads (Millipore) were used to pulldown the antibody. DNA was eluted (1% SDS; 100 mM $NaHCO_3$), followed by reversion of the crosslink RNaseA (Thermo Fisher Scientific) and proteinase K (Finnzymes Diagnostics) treatment. DNA was purified using the QIAquick PCR purification kit (Qiagen) and qPCR was performed with corresponding primers under following cycling conditions: 95 °C for 3 min, followed by 40 cycles of 95 °C for 3 sec. and 60 °C for 30 sec, finishing at 65 ºC for 5 sec. The values were adjusted to the IgG control (subtraction) and calculated as a ratio to the input (normalization); the data were presented as fold change to siControl.

RNA immunoprecipitation

Cells were cultured for 48 hours, scraped and harvested in PBS, and lysed in lysis buffer (150 mM NaCl, 50 mM Tris pH8.0, 1% NP40 with PhosphoSTOP, Sigma-Aldrich) for 15 min on ice while vortexed every 5 min. Samples were sonicated 3x15 sec using Bioruptor Sonicator (Diagenode) and centrifuged at 1500 rpm for 5 min. Supernatant was collected and protein concentration measured using colorimetric Bradford assay (BioRad). A volume corresponding to 1 mg protein was rotated with anti-CTCF antibody (Cell Signaling, Cat# 2899) and Salmon sperm DNA/protein A Agarose beads (Millipore) overnight. Beads were washed in RIPA buffer (50 mM Tris-HCL pH 7.4, 1% NP40, 0.5% $C_{24}H_{40}O_4$, 150 mM SDS, 2 nM EDTA), and

1 ml of TRIZOL was added to the beads and RNA was isolated using Nucleospin kit II.

Colony formation assay

One thousand cells per well plated onto six-well plates were transfected with either control siRNA or siRNA against *CEBPB-AS1* for 48 h and then retransfected for another 48 h. Colonies were grown for 4–5 days, with media change every 2 days. Cells were fixed using 4% buffered formaldehyde, stained with 0.05% crystal violet, and plates were scanned using Epson scanner V370. To estimate number of colonies, crystal violet staining was dissolved in 100% methanol, diluted to 1:10 in PBS and absorbance was measured at 540 nM using Tecan Spark 10M plate reader instrument.

Annexin V-PI detection by flow cytometry

A375 and A375PR1 cells transfected and treated with vemurafenib, were collected in 100 µL fluorescence-activated cell sorting (FACS) incubation buffer (10 mM HEPES/NaOH, pH 7.4, 140 mM NaCl, 5 mM $CaCl_2$), containing 1% Annexin V FLOUS (Roche Molecular Biochemicals, Penzberg, Germany) and 500 µg/µl propidium iodide (PI; Sigma-Aldrich). Annexin V and PI stained cells were assessed in an ACEA Biosciences NovoCyte Flow Cytometer. A minimum of 10 000 cells were gated for each sample.

RNA expression data

We downloaded read count data from 473 primary and metastatic CMM samples from the Cancer Genome Atlas (TCGA) project, and homogenously processed and annotated using Gencode version 25 through recount2 [15], normalized by trimmed mean of M-values [16] and transformed to log2 counts per million mapped reads using limma-voom before further analysis [17]. Spearman´s rank correlation was used to correlate the expression values between *CEBPB* and *CEBPB-AS1*. Cox proportional hazards was used to calculate correlation to overall survival (OS), and visualized by Kaplan–Meier plots with patients stratified by low, medium or high gene expression.

CEBPB mRNA expression data was extracted from previously obtained targeted sequencing of RNA from CMM fine needle aspiration samples using Ion AmpliSeq as described [13,18].

Statistical analysis

Data were presented as mean ± SEM, unless stated otherwise. Statistical analysis was performed using a Student's *t*-test and values of $*P < 0.05$ or $**P < 0.01$ or $***P < 0.005$ were considered statistically significant.

Results

Correlation between CEBPB mRNA levels and survival of cutaneous malignant melanoma patients

In order to determine whether CEBPB is involved in the survival or the treatment outcome of CMM patients, we have analyzed the mRNA expression data in two data sets: TCGA database and our own AmpliSeq data obtained from a cohort of CMM patients treated with BRAFi [13,18]. Analysis of the TCGA database revealed a positive correlation between higher CEBPB mRNA expression and longer OS (Fig. 1a). Analysis of our AmpliSeq data showed a correlation between higher CEBPB mRNA levels in pretreated tumor cells and a longer PFS for CMM patients treated with BRAFi's (Fig. 1b). The analysis of these two data sets, thus, suggested that CEBPB may play a role in the CMM patients' OS and the response to the mutant BRAF-targeting therapy.

Characterization of CEBPB-AS1 transcript

The possible involvement of CEBPB in sensitivity to therapy prompted us to investigate how *CEBPB* expression may be regulated in CMM cells. Antisense transcripts originate from a majority of coding genes' loci and have been shown to regulate gene transcription of their sense counterparts [5]. Therefore, we searched the University of California, Santa Cruz (UCSC) genome browser for an antisense transcript to the CEBPB transcript and identified *CEBPB-AS1* that partially overlaps in a head-to-head orientation with the *CEBPB* transcript (Fig. 2a). Aiming at characterizing this transcript, we used cell fractionation, poly(A) depletion and RNA-stability experiments, which revealed that *CEBPB-AS1* was expressed in both nuclear and cytoplasmic fractions similarly to *CEBPB* mRNA (Fig. 2b). In addition, *CEBPB-AS1* is a polyadenylated transcript (Fig. 2c) and has a half-life of more than 10 h (as compared to *CEBPB* that had a higher turnover rate, Fig. 2d). Next, we used a pair of CMM cell lines, A375 and its BRAFi resistant sub-line, A375 PR1 [13]. Using primer walk with different sets of primers (Fig. 2e), in these two CMM cell lines we confirmed the length of the 5′UTR of *CEBPB* to be the same as annotated in the UCSC genome browser (Fig. 2f). A CEBPB binding site can be found in a region upstream of the transcriptional start site of *CEBPB-AS1* (Fig. 2a). Indeed, silencing of CEBPB led to decreased expression of *CEBPB-AS1* in the A375 and the A375PR1 cell lines (Fig. 2g and h) suggesting that CEBPB may regulate the expression of this antisense transcript. Thus, we have confirmed and further characterized a stable polyadenylated antisense RNA partially overlapping with the *CEBPB* transcript, that is present in both the nucleus and the cytoplasm and can be positively regulated by CEBPB in CMM cell lines.

Silencing of CEBPB-AS1 upregulates CEBPB expression and CEBPB binding to DNA

In order to investigate if *CEBPB-AS1* can regulate CEBPB expression, we knocked down *CEBPB-AS1* in a panel of CMM cell lines. Albeit with a different efficiency, the knockdown led to a significantly increased mRNA expression of *CEBPB* in CMM cell lines

Fig. 1

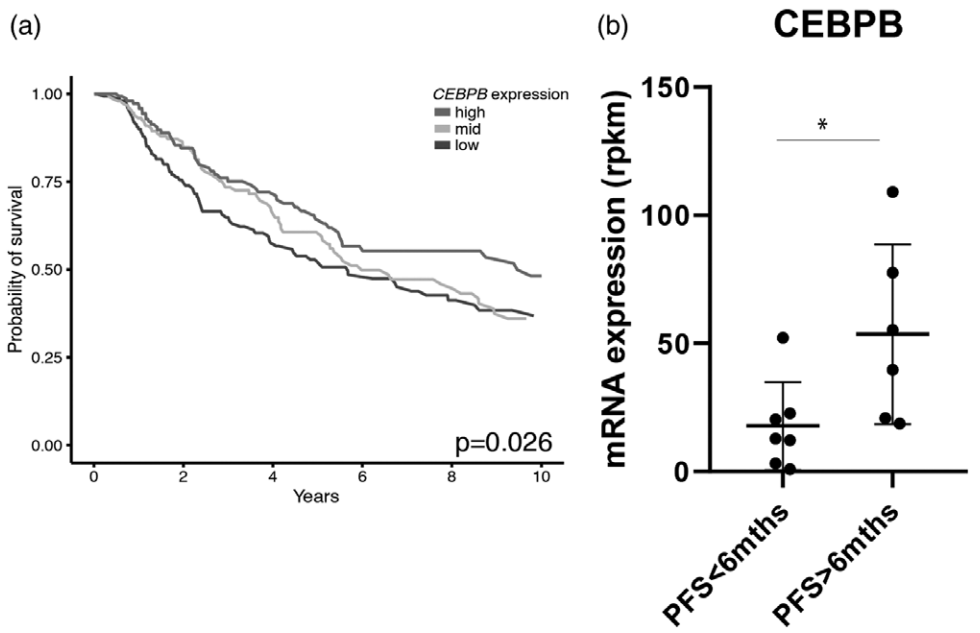

Correlation between *CEBPB* mRNA levels and survival of CMM patients. (a) Kaplan–Meier plot showing overall survival of 473 patients with CMM (TCGA), stratified by *CEBPB* gene expression (low, medium, high as black, light and dark gray, respectively). Cox proportional hazard regression of overall survival vs. *CEBPB* expression coefficient −0.177, $P = 0.026$. (b) *CEBPB* mRNA analysis from the AmpliSEQ data from tumors from CMM patients (n = 13) prior receiving targeted BRAFi–based therapy (Table 1; raw data published elsewhere). Patients were divided according to their PFS using 6 months as a cutoff, $*p = 0.036$. BRAFi, BRAF-inhibitor; CMM, cutaneous malignant melanoma; PFS, progression-free survival; TCGA, the Cancer Genome Atlas.

(Fig. 3a–f). A similar result was obtained using different siRNA targeting *CEBPB-AS1* in A375 and A375 PR1 cell lines (Supplementary Figure 1, Supplemental digital content 1, *http://links.lww.com/MR/A233*). The effect of *CEBPB-AS1* knockdown on CEBPB protein expression was also verified by Western blotting (Fig. 3g). CEBPB can bind in its own regulatory region (Fig. 2a), and it was previously published that CEBPB can regulate its own transcription [19]. Notably, knockdown of *CEBPB-AS1* increased the binding of CEBPB to its own and to the *CEBPB-AS1* regulatory regions [Fig. 3h and i; location of primers for chromatin immunoprecipitation (ChIP) in Supplementary Figure 2A, Supplemental digital content 1, *http://links.lww.com/MR/A233*]. Thus, *CEBPB-AS1* can negatively regulate *CEBPB* mRNA and consequently protein expression, and the CEBPB activity in binding to the promoter regions.

CEBPB-AS1 mediates epigenetic modifications in the CEBPB regulatory region

In order to understand the mechanism of *CEBPB-AS1*-mediated effects on *CEBPB* transcription, we asked whether the former can modulate the epigenetic status of the regulatory region upstream of the *CEBPB* gene. Antisense RNAs have been shown to be capable of recruiting or evicting chromatin-modifying proteins to/from DNA regions [20]. One such protein is CCCTC-binding factor (CTCF) involved in both activation and repression of transcription, in regulating 3D structure of chromatin, and also to be able to bind to lncRNA [21]. RNA immunoprecipitation revealed that *CEBPB-AS1* can bind to CTCF (Fig. 4a). The ChIP-data from the UCSC genome browser showed two different binding sites for CTCF in the *CEBPB* regulatory region (Supplementary Figure 2B, Supplemental digital content 1, *http://links.lww.com/MR/A233*). ChIP assay showed that knockdown of *CEBPB-AS1* led to a decreased CTCF binding to this region (Fig. 4b) suggesting that CTCF may bind to this region through *CEBPB-AS1*. Due to CTCF involvement in the regulation of chromatic structure, we assessed the trimethylation of histone H3 at lysine 27 (H3K27me3) by ChIP and found it to be significantly enriched in this region upon *CEBPB-AS1* knockdown (Fig. 4c). Also, EZH2, that catalyzes the methylation of histone H3 at lysine 27, showed enrichment at the same region upon *CEBPB-AS1* knockdown (1.6-, 1.9- and 4.3-fold enrichment in three independent experiment; Fig. 4d). Furthermore, using a methyl-cytosine-specific McrBc enzyme that specifically cuts methylated DNA, we found that *CEBPB-AS1* knockdown in either A375 or A375PR1 cells resulted in an increased DNA methylation at the same *CEBPB* regulatory region (Supplementary Figure 3, Supplemental digital content 1, *http://links.lww.com/MR/A233*). These data together indicated a silencing of the

Fig. 2

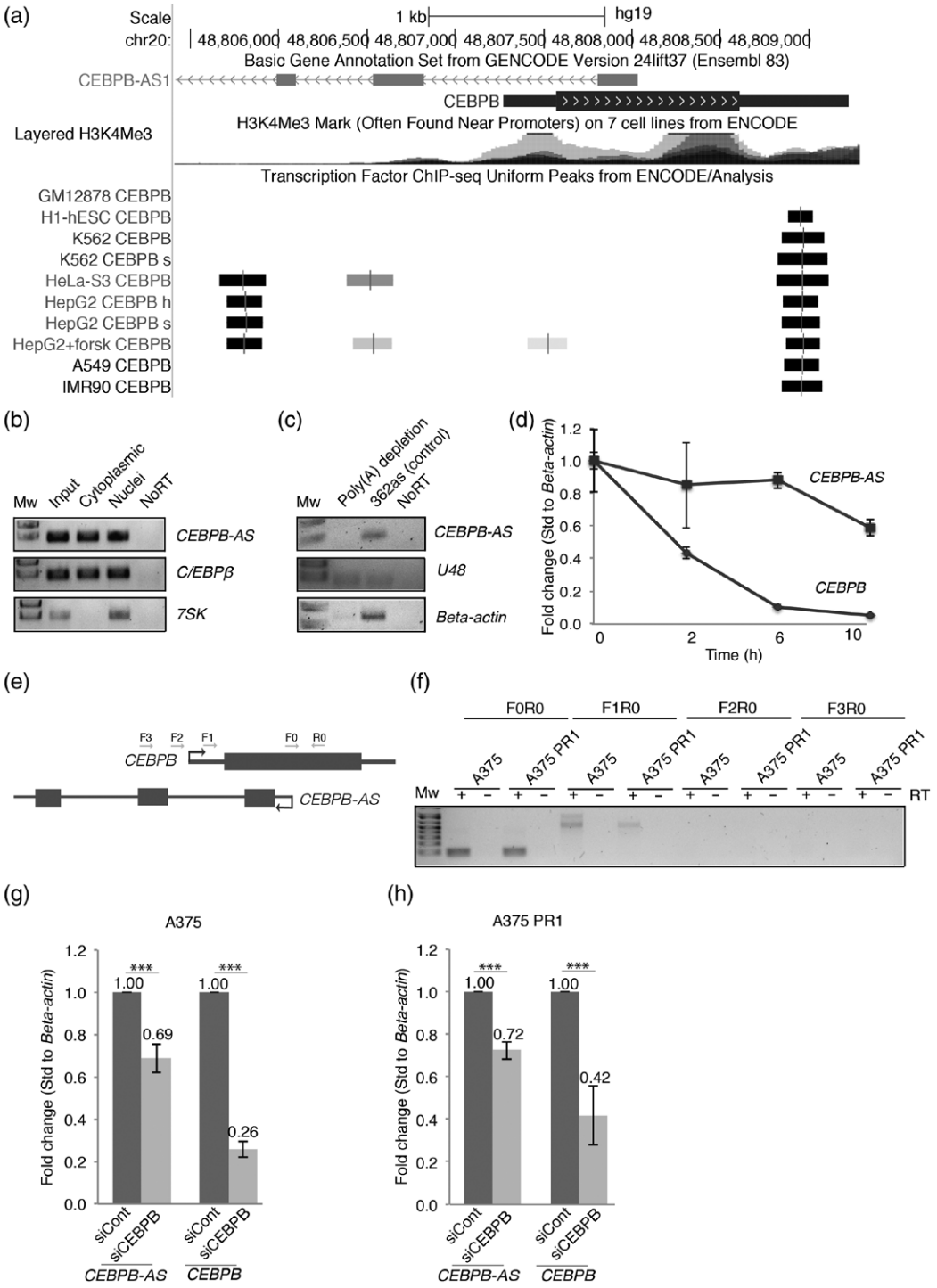

Characterization of *CEBPB-AS1* transcript. (a) A schematic depiction of ChIP-seq data from the UCSC genome browser showing enrichment of CEBPB in the *CEBPB* and *CEBPB-AS1* regulatory regions. H3K4me3 shows two peaks within the CEBPB locus. Gray boxes – peak clusters of transcription factor occupancy. Darkness of the box is proportional to the signal strength. (b) RNA was extracted from the cytoplasmic and nuclear fraction of A375PR1 and semi-qRT-PCR was performed to detect *CEBPB-AS1* and *CEBPB* transcripts. 7SK – a known nuclear transcript. (c) *CEBPB-AS1* expression was determined by semi-qRT-PCR in the control (362as) and poly(A)-depleted fractions of HEK293T cells. U48 and beta-actin were used as a positive control for non-polyadenylated and polyadenylated transcript, respectively. (d) RNA stability of *CEBPB* and *CEBPB-AS1* was measured in A375R1 cells at indicated time points using qRT-PCR after blocking transcription with Actinomycin D; a representative of two independent experiments, each performed in triplicate, is shown. (e) Location of the primer sets used in the primer walk (f) to determine the 5′ end of *CEBPB-AS* transcript in A375 and A375PR1 cell lines. See Supplementary Table 1, Supplemental digital content 1, *http://links.lww.com/MR/A233* for primers. The results allowed designing siRNA against *CEBPB-AS1* that would specifically target this transcript. (g and h) Expression of *CEBPB-AS1* and *CEBPB* measured by qRT-PCR after siRNA knockdown of *CEBPB* in A375 (g) and A375 PR1 (h) cells. Data from three independent experiments (n = 3) represent mean ± SEM. semi-qRT-PCR, semi-quantitative reverse transcription PCR; UCSC, University of California, Santa Cruz.

Fig. 3

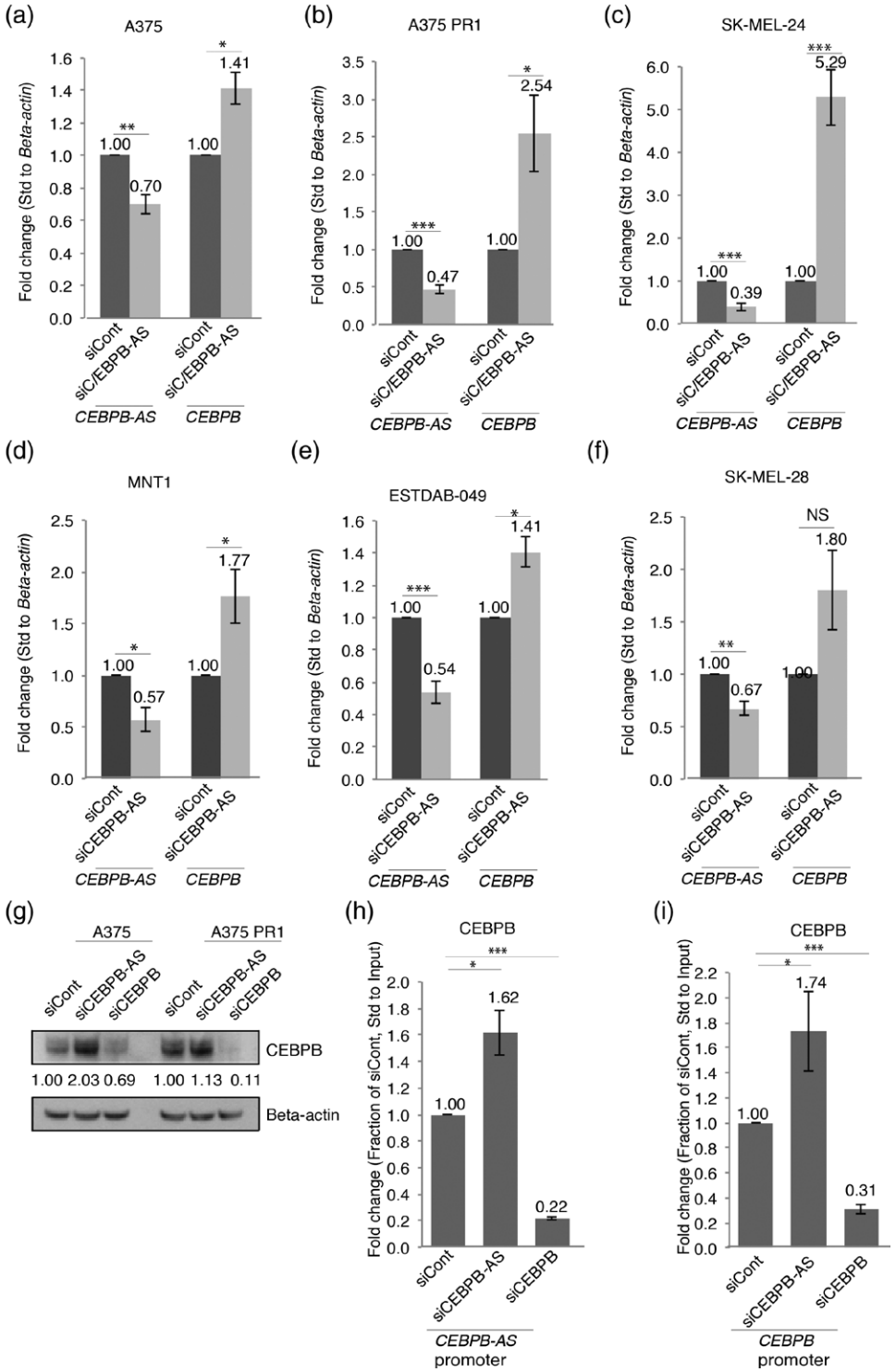

Silencing of *CEBPB-AS1* upregulates CEBPB expression. (a–f) Six CMM cell lines were transfected with siRNA targeting *CEBPB-AS1* for 48 h and evaluated for *CEBPB-AS1* and *CEBPB* RNA expression by qRT-PCR. Data from three independent experiments (n = 3) represent mean ± SEM. (g) Western blot analysis of CEBPB protein expression after siRNA-mediated knockdown of either *CEBPB-AS1* or *CEBPB* in the A375 and A375PR1 cell lines. The protein levels of CEBPB were quantified, normalized to beta-actin and shown as fold change to the siControl. (h and i) ChIP using antibodies against CEBPB and qPCR of the CEBPB regulatory regions in *CEBPB-AS1* (h; independent experiments n = 4) and *CEBPB* (i; independent experiments n = 3) promoters in A375PR1 cells transfected with either siControl or siCEBPB-AS1. Primers are depicted in Supplementary Figure 2A, Supplemental digital content 1, *http://links.lww.com/MR/A233*. The plots represent fold change to siControl, adjusted to the IgG control and normalized to the input. Data represent mean ± SEM. *$p < 0.05$, **$p < 0.01$, ***$p < 0.005$. ChIP, chromatin immunoprecipitation; CMM, cutaneous malignant melanoma.

Fig. 4

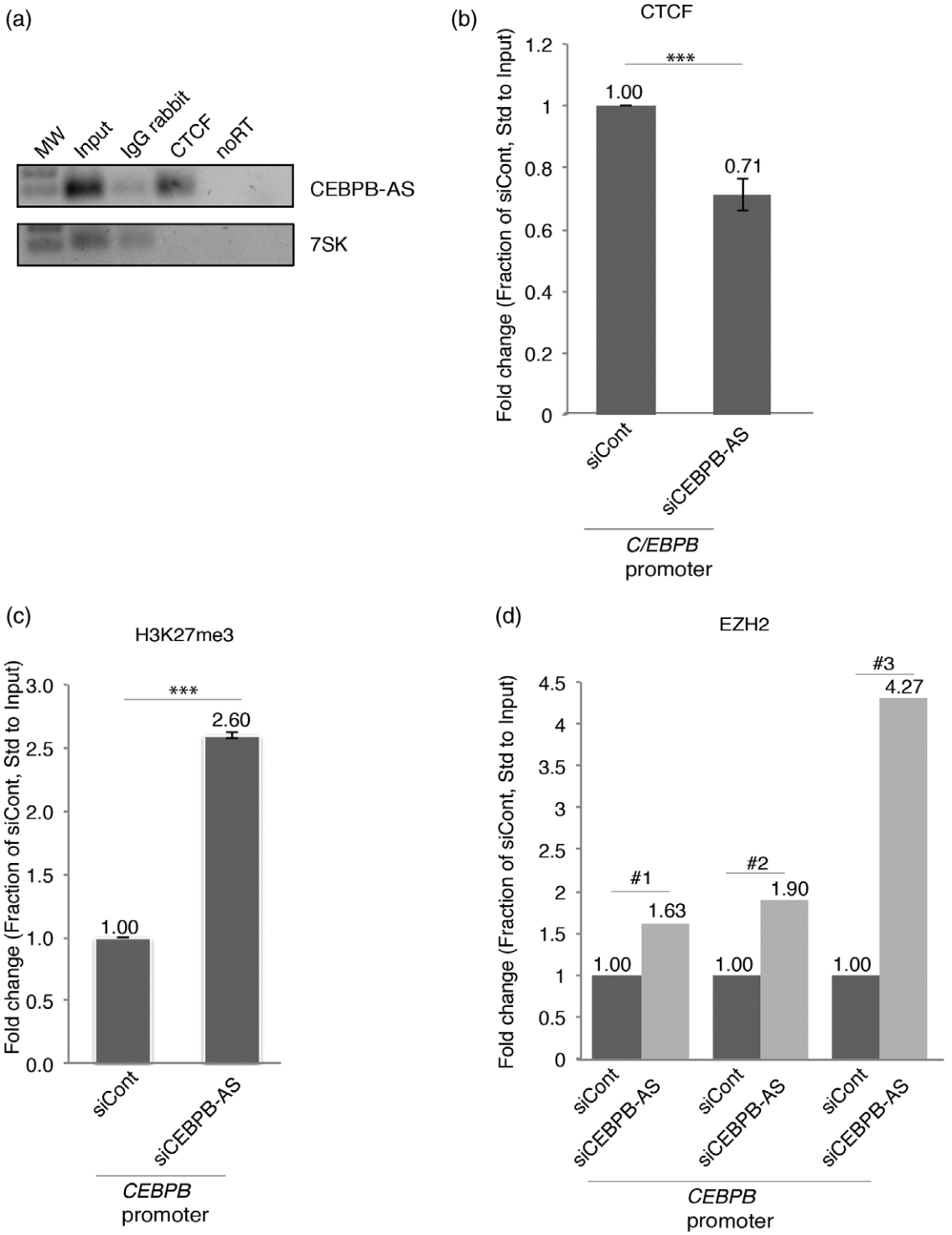

Silencing of *CEBPB-AS1* results in epigenetic modifications at the CEBPB regulatory region. (a) RNA-IP (RIP) was performed in A375PR1 cells using antibodies against CTCF. The *CEBPB-AS1* transcript was detected using semi-qRT-PCR. (b–d) The A375PR1 cells were transfected with either siControl or siCEBPB-AS1 and ChIP was performed using antibodies against CTCF (b), H3K27me3 (c) and EZH2 (d). Primers in the regulatory region of *CEBPB* were used for qPCR; independent experiments n = 3. Data represent mean ± SEM. ***$p < 0.005$. For EZH2, due to variations between the experiments, statistical significance was not reached, and results from individual experiments are shown. Each value was first adjusted to the IgG control by subtraction, calculated as a ratio to the input (normalization), and the data are presented as fold change to siControl. ChIP, chromatin immunoprecipitation; RIP, RNA immunoprecipitation; semi-qRT-PCR, semi-quantitative reverse transcription PCR.

chromatin upon *CEBPB-AS1* knockdown. Interestingly, CEBPB is known to bind to methylated DNA regions and not repressing but activating gene transcription [9,10]. Thus, knockdown of *CEBPB-AS1* resulted in a state of the chromatin normally associated with gene repression, in this case, however, leading to an increased binding of CEBPB to DNA. In conclusion, our data suggested that *CEBPB-AS1* may tether CTCF to the CEBPB regulatory region resulting in the opening of the chromatin, which, due to specific features of CEBPB, leads to a decreased affinity of this TF to its own promoter sequence and consequently, to a decrease in CEBPB expression.

Silencing of *CEBPB-AS1* decreases cutaneous malignant melanoma cell proliferation and sensitizes cutaneous malignant melanoma cells to BRAF-inhibitor vemurafenib

As our experiments demonstrated, *CEBPB* levels were increased by knocking down *CEBPB-AS1*. To assess the biological effect of this increase, we used a colony formation assay to follow cell proliferation for a longer period of time. A knockdown of *CEBPB-AS1* using two concentrations of siRNA in A375 and A375PR1 CMM cells led to a decrease in colony formation in A375 cells, and even more significant – in the resistant A375PR1 cell line (Fig. 5a, b, d and e). Similar result was obtained in MNT1 cell line (Fig. 5c and f). Since our data from a cohort of patients treated with BRAF-targeting therapy pointed at a significantly longer PFS for patients with higher CEBPB expression in their pretreatment CMM cells (Fig. 1b), we asked whether increasing CEBPB expression through manipulating *CEBPB-AS1* in CMM cell lines would affect their response to the drug. For this, we used FACS analysis of AnnexinV/PI stained cells of two melanoma cell lines and their vemurafenib-resistant derivatives to monitor the apoptotic response after drug treatment. siRNA-mediated knockdown of *CEBPB-AS1* in the parental A375 and the vemurafenib-resistant A375PR1 treated with two different concentrations of vemurafenib resulted in a significantly increased cell death as compared to the siControl transfected cells (Fig. 5g) with somewhat more pronounced effect in the resistant sub-line (Fig. 5g, right graph). Similarly, in both the parental MNT1 and the dabrafenib/vemurafenib-resistant MNT1-DR100, knockdown of *CEBPB-AS1* potentiated the proapoptotic effect of vemurafenib (Fig. 5h). This data indicates that a knockdown of *CEBPB-AS1* can affect CMM cell proliferation and sensitize resistant CMM cells to the BRAFi vemurafenib-induced apoptosis.

Discussion

The involvement of CEBPB in cancer development is controversial and most probably depends on many factors, which are still poorly understood [8]. Our data analysis using the TCGA database and our own AmpliSeq data from CMM tumors suggested that higher *CEBPB* levels may represent a novel prognostic marker, in particular, in patients treated with BRAF-targeting therapy. This is the first report, to our knowledge, that pointed at the connection between CEBPB and sensitivity of CMM tumors to the mutant BRAF-targeting therapy. We also attempted to correlate CEBPB mRNA expression levels to the treatment outcome using available published studies on patients' cohorts treated with MAPK pathway-targeting drugs [22,23]. In one study, CEBPB expression levels did not differ between complete responders and non-responders (as based on the authors' data analysis) [23], while in another study, although based on three tumor samples, high CEBPB levels were found only in the sample from a patient with a longest PFS ([22], GSE50535, data not shown). Thus bioinformatics analysis of RNAseq data from more patients' cohorts published in the future will help to validate and better understand this relationship.

Searching for a novel molecular mechanism, we found and for the first time characterized an antisense RNA, *CEBPB-AS1*, that is involved in fine-tuning the regulation of *CEBPB* transcriptional levels. Moreover, by silencing *CEBPB-AS1* in the BRAFi-sensitive and the corresponding resistant sub-lines, we could indirectly affect CEBPB expression and increase the sensitivity to BRAFi-induced antitumor effects in CMM cell lines. In this study, we could not assess the impact of a direct manipulation of CEBPB levels on colony formation or on the apoptotic response to BRAFis due to a variability of cellular response to the knockdown of CEBPB in different cell lines (data not shown). This could be due to differential expression and distinct role of CEBPB isoforms or of CEBPB levels for cancer cell proliferation or survival [8]. Also a knock-down of *CEBPB* will result in downregulation of *CEBPB-AS1* thus leading to opposing stimuli (see below). On the other hand, knockdown of *CEBPB-AS1* reproducibly both stabilized CEBPB levels and decreased proliferation of melanoma cell lines, and sensitized cells to BRAFi's mediated loss of viability. Thus, manipulation of the levels of this stable antisense RNA rather than of CEBPB itself may represent a valid strategy to sensitize CMM to the BRAFi-based therapy. Although there are still only few preclinical reports on targeting lncRNAs [24], this may represent a viable strategy in anti-cancer therapy. Since antisense RNAs are very common: about 2/3 of protein-coding genes in the mammalian genome have an antisense counterpart [25], investigating their mechanism of action, specifically on their sense counterparts that they overlap with, and their role in cancer and therapy resistance may show very useful in looking for biomarkers and designing novel therapeutic approaches.

Mechanistically, our data suggest that CEBPB drives transcription of *CEBPB-AS*, while latter in turn negatively regulates the transcription and activity of *CEBPB*.

Fig. 5

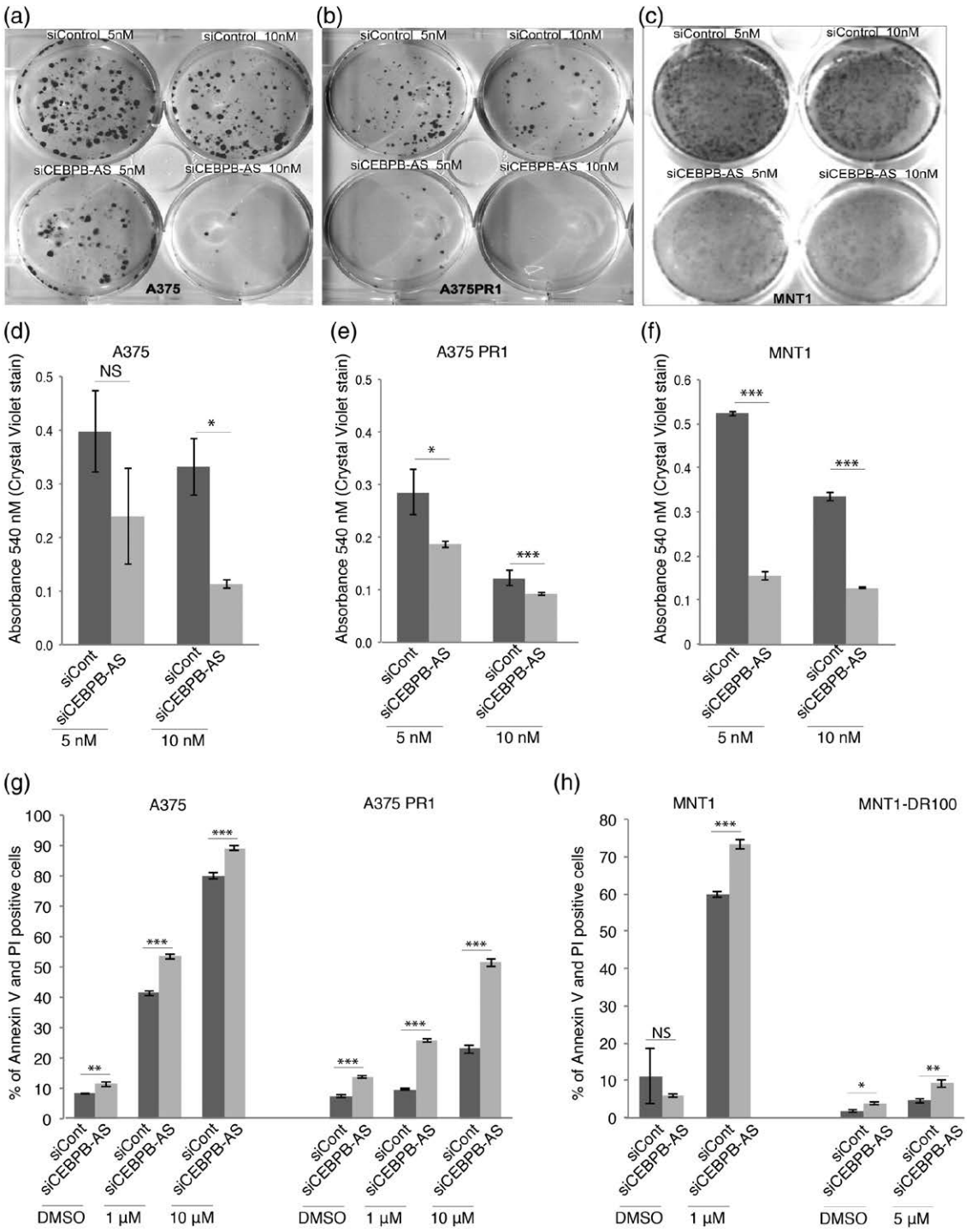

Silencing of *CEBPB-AS1* affects CMM cell line proliferation and sensitizes CMM cells to BRAF-inhibitor vemurafenib. (a–f) A375, A375PR1 or MNT1 cell lines were transfected with siRNA against *CEBPB-AS1* (siCEBPB-AS1) and colony formation assay was performed; (a–c) representative images and (d–f) measurements of the crystal violet stain that is proportional to the number of colonies/cells per plate; independent experiments n = 3. (g) A375 or A375PR1 cell lines were transfected as in (a and b), treated with either 1 or 10 μM of vemurafenib and induction of cell death was analyzed using Annexin V and propidium iodide (PI) staining and FACS; data from one of three independent experiments represent percent of all Annexin V positive cells, including PI-positive; technical replicates n = 3. ***$p < 0.005$, *$p < 0.05$. (h) MNT1 or MNT1-DR100 cell lines were transfected as in (g), treated with the indicated concentrations of vemutafenib and cell death was analyzed as in (g); data from two independent experiments are presented, each in at least two technical replicates. CMM, cutaneous malignant melanoma; FACS, fluorescence-activated cell sorting.

Taken into account that CEBPB can regulate its own transcription [19], this may provide a negative feedback loop that are known to be involved in shutting down signaling or fine-tuning gene transcription. This data allows us to speculate that a knock-down of antisense RNA would directly disrupt the negative feedback loop that regulates CEBP expression leading to somewhat stabilized CEBPB levels. Antisense RNA may regulate sense gene transcription in different ways, one of which can be a direct interference with the process of transcription. In this study, we have investigated another mechanism, namely epigenetic changes afflicted through the silencing of *CEBPB-AS1*. Based on our data, we hypothesize that *CEBPB-AS1* through the binding to a highly conserved zinc finger protein CTCF and its recruitment to the promoter of *CEBPB* can promote a discharge of CEBPB from this region and a decrease in *CEBPB* transcription. In line with our data, CTCF depletion has been shown to upregulate CEBPB [26] implicating its involvement in the regulation of CEBPB transcription. At the same time, we and others have shown that lncRNAs are capable of facilitating recruitment or eviction of epigenetic modifying proteins at specific gene loci [5,21,27], and, thus, our new data add *CEBPB-AS1* to this list of lncRNAs.

CTCF was shown to be one of the factors capable of opening up compact chromatin and resulting in a decrease in the H3K27me3 mark [28]. Indeed, silencing of *CEBPB-AS1* and a decrease in CTCF binding that we observed resulted in a state of chromatin that is usually associated with gene repression, namely increased H3K27me3, recruitment of EZH2 as well as DNA methylation at the CEBPB regulatory region. Notably, CEBPB is one of the few TFs with an enhanced binding affinity towards methylated CRE and CEBPB DNA motifs resulting in activation of gene transcription [9,10,29,30]. Methylation of CpG islands enhances the binding of CEBPB while binding of other TFs was inhibited [9,10]. Thus, our results are in concordance with previously published studies and show that CEBPB binding to its own promoter region is associated with a 'condensed' epigenetic state.

In conclusion, we found CEBPB involvement in the sensitivity of CMM tumors to the BRAFi-based therapy and present a novel mode of regulation of CEBPB levels and activity by its antisense transcript, *CEBPB-AS1*. This data implies that manipulating *CEBPB-AS1* may represent a new approach of sensitizing CMM tumors for BRAFi-based therapy.

Acknowledgements

We thank Fernanda Costa Svedman for clinical follow-up data and Karl-Johan Ekdahl for assistance with clinical samples. Professor Dan Grandér, who was the grant holder and the senior author of this project at the Department of Oncology & Pathology, passed away in October 2017. We are deeply sorrowed by his tragic death and dedicate this study to his memory.

This work was supported by Cancerfonden, CF (CAN 2015/698 to D.G.; CAN 2017/733 to J.H.) and Radiumhemmets Research funds (N 170207 and N 174122 to D.G.; 174153 to J.H.).

Conflicts of interest

There are no conflicts of interest.

References

1 Flaherty KT, Puzanov I, Kim KB, Ribas A, McArthur GA, Sosman JA, *et al.* Inhibition of mutated, activated BRAF in metastatic melanoma. *N Engl J Med* 2010; **363**:809–819.
2 Sosman JA, Kim KB, Schuchter L, Gonzalez R, Pavlick AC, Weber JS, *et al.* Survival in BRAF V600-mutant advanced melanoma treated with vemurafenib. *N Engl J Med* 2012; **366**:707–714.
3 Long GV, Stroyakovskiy D, Gogas H, Levchenko E, de Braud F, Larkin J, *et al.* Combined BRAF and MEK inhibition versus BRAF inhibition alone in melanoma. *N Engl J Med* 2014; **371**:1877–1888.
4 Kakadia S, Yarlagadda N, Awad R, Kundranda M, Niu J, Naraev B, *et al.* Mechanisms of resistance to BRAF and MEK inhibitors and clinical update of US Food and Drug Administration-approved targeted therapy in advanced melanoma. *Onco Targets Ther* 2018; **11**:7095–7107.
5 Johnsson P, Ackley A, Vidarsdottir L, Lui WO, Corcoran M, Grandér D, Morris KV. A pseudogene long-noncoding-RNA network regulates PTEN transcription and translation in human cells. *Nat Struct Mol Biol* 2013; **20**:440–446.
6 Riganti C, Kopecka J, Panada E, Barak S, Rubinstein M. The role of C/EBP-beta LIP in multidrug resistance. *J Natl Cancer Inst* 2015; **107**:djv046.
7 Cerezo M, Lehraiki A, Millet A, Rouaud F, Plaisant M, Jaune E, *et al.* Compounds triggering ER stress exert anti-melanoma effects and overcome BRAF inhibitor resistance. *Cancer Cell* 2016; **29**:805–819.
8 Sebastian T, Johnson PF. Stop and go: anti-proliferative and mitogenic functions of the transcription factor C/EBPbeta. *Cell Cycle* 2006; **5**:953–957.
9 Rishi V, Bhattacharya P, Chatterjee R, Rozenberg J, Zhao J, Glass K, *et al.* CpG methylation of half-CRE sequences creates C/EBPalpha binding sites that activate some tissue-specific genes. *Proc Natl Acad Sci U S A* 2010; **107**:20311–20316.
10 Mann IK, Chatterjee R, Zhao J, He X, Weirauch MT, Hughes TR, Vinson C. CG methylated microarrays identify a novel methylated sequence bound by the CEBPB|ATF4 heterodimer that is active in vivo. *Genome Res* 2013; **23**:988–997.
11 Zahnow CA. CCAAT/enhancer-binding protein beta: its role in breast cancer and associations with receptor tyrosine kinases. *Expert Rev Mol Med* 2009; **11**:e12.
12 Cuomo M, Nicotra MR, Apollonj C, Fraioli R, Giacomini P, Natali PG. Production and characterization of the murine monoclonal antibody 2G10 to a human T4-tyrosinase epitope. *J Invest Dermatol* 1991; **96**:446–451.
13 Azimi A, Tuominen R, Costa Svedman F, Caramuta S, Pernemalm M, Frostvik Stolt M, *et al.* Silencing FLI or targeting CD13/ANPEP lead to dephosphorylation of EPHA2, a mediator of BRAF inhibitor resistance, and induce growth arrest or apoptosis in melanoma cells. *Cell Death Dis* 2017; **8**:e3029.
14 Azimi A, Caramuta S, Seashore-Ludlow B, Boström J, Robinson JL, Edfors F, *et al.* Targeting CDK2 overcomes melanoma resistance against BRAF and Hsp90 inhibitors. *Mol Syst Biol* 2018; **14**:e7858.
15 Collado-Torres L, Nellore A, Kammers K, Ellis SE, Taub MA, Hansen KD, *et al.* Reproducible RNA-seq analysis using recount2. *Nat Biotechnol* 2017; **35**:319–321.
16 Robinson MD, Oshlack A. A scaling normalization method for differential expression analysis of RNA-seq data. *Genome Biol* 2010; **11**:R25.
17 Law CW, Chen Y, Shi W, Smyth GK. voom: Precision weights unlock linear model analysis tools for RNA-seq read counts. *Genome Biol* 2014; **15**:R29.
18 Das I, Wilhelm M, Höiom V, Franco Marquez R, Costa Svedman F, Hansson J, *et al.* Combining ERBB family and MET inhibitors is an effective therapeutic strategy in cutaneous malignant melanoma independent of BRAF/NRAS mutation status. *Cell Death Dis* 2019; **10**:663.

19 Ramji DP, Foka P. CCAAT/enhancer-binding proteins: structure, function and regulation. *Biochem J* 2002; **365**:561–575.
20 Yap KL, Li S, Muñoz-Cabello AM, Raguz S, Zeng L, Mujtaba S, *et al*. Molecular interplay of the noncoding RNA ANRIL and methylated histone H3 lysine 27 by polycomb CBX7 in transcriptional silencing of INK4a. *Mol Cell* 2010; **38**:662–674.
21 Sun S, Del Rosario BC, Szanto A, Ogawa Y, Jeon Y, Lee JT. Jpx RNA activates Xist by evicting CTCF. *Cell* 2013; **153**:1537–1551.
22 Sun C, Wang L, Huang S, Heynen GJ, Prahallad A, Robert C, *et al*. Reversible and adaptive resistance to BRAF(V600E) inhibition in melanoma. *Nature* 2014; **508**:118–122.
23 Yan Y, Wongchenko MJ, Robert C, Larkin J, Ascierto PA, Dréno B, *et al*. Genomic features of exceptional response in vemurafenib ± cobimetinib-treated Patients with BRAFV600-mutated metastatic melanoma. *Clin Cancer Res* 2019; **25**:3239–3246.
24 Richtig G, Ehall B, Richtig E, Aigelsreiter A, Gutschner T, Pichler M. Function and clinical implications of long non-coding RNAs in Melanoma. *Int J Mol Sci.* 2017; **18**:E715.
25 Yelin R, Dahary D, Sorek R, Levanon EY, Goldstein O, Shoshan A, *et al*. Widespread occurrence of antisense transcription in the human genome. *Nat Biotechnol* 2003; **21**:379–386.
26 Lefevre P, Witham J, Lacroix CE, Cockerill PN, Bonifer C. The LPS-induced transcriptional upregulation of the chicken lysozyme locus involves CTCF eviction and noncoding RNA transcription. *Mol Cell* 2008; **32**:129–139.
27 Chen WM, Chen WD, Jiang XM, Jia XF, Wang HM, Zhang QJ, *et al*. HOX transcript antisense intergenic RNA represses E-cadherin expression by binding to EZH2 in gastric cancer. *World J Gastroenterol* 2017; **23**:6100–6110.
28 Weth O, Paprotka C, Günther K, Schulte A, Baierl M, Leers J, *et al*. CTCF induces histone variant incorporation, erases the H3K27me3 histone mark and opens chromatin. *Nucleic Acids Res* 2014; **42**:11941–11951.
29 Irizarry RA, Ladd-Acosta C, Wen B, Wu Z, Montano C, Onyango P, *et al*. The human colon cancer methylome shows similar hypo- and hypermethylation at conserved tissue-specific CpG island shores. *Nat Genet* 2009; **41**:178–186.
30 Niesen MI, Osborne AR, Yang H, Rastogi S, Chellappan S, Cheng JQ, *et al*. Activation of a methylated promoter mediated by a sequence-specific DNA-binding protein, RFX. *J Biol Chem* 2005; **280**:38914–38922.